A numerical study on unsteady natural convection of air with variable viscosity over an isothermal vertical cylinder

Hari Ponnamma Rani* and Chang Nyung Kim**,***,†

*Department of Mathematics and Humanities, National Institute of Technology, Warangal, India
**Department of Mechanical Engineering, College of Advanced Technology, Kyung Hee University, Korea
***Industrial Liaison Research Institute, Kyung Hee, Korea

Abstract−The present study deals with the boundary layer flow and heat transfer of unsteady laminar free convection flow past a semi-infinite isothermal vertical cylinder immersed in air. The fluid viscosity is assumed to vary with the temperature. An implicit finite-difference method has been employed to solve the governing non-dimensional boundary layer equations. A parametric study is performed to illustrate the influence of variable viscosity on the velocity and temperature profiles. The numerical results reveal that the viscosity has significant influences on the transient velocity and temperature profiles, average skin-friction coefficient and the average heat transfer rate. The results indicate that as the viscosity parameter increases, the temperature and the skin-friction coefficient increase, while the velocity near the wall and the Nusselt number decrease.

Key words: Transient, Natural Convection, Vertical Cylinder, Variable Viscosity, Finite Difference Method

INTRODUCTION

The transient natural convection flows over vertical bodies have a wide range of applications in engineering and technology. These kinds of problems are frequently encountered in the study of enhanced heat transfer around various kinds of electrical and electronic devices and nuclear reactors. In manufacturing processes such as hot extrusion, metal forming and crystal growing, heat transfer effects plays an important role. In particular, the study of enhanced heat transfer is very useful in cylindrical surfaces. Free convection flow of air bathing a vertical cylinder with a prescribed surface temperature was first presented by Sparrow and Gregg [1] by applying the similarity method and power series expansion. Later on, Minkowycz and Sparrow [2] obtained a solution for the same problem using the non-similarity method. Fujii and Uehara [3] analyzed the local heat transfer results for arbitrary Prandtl numbers. Lee et al. [4] investigated the problem of natural convection in laminar boundary layer flow along slender vertical cylinders and needles for the power-law variation in wall temperature. Dring and Gebhart [5] presented the transient natural convection results in association with the thin wires in liquids. Velusamy and Garg [6] presented the numerical solution for transient natural convection over heat generating vertical cylinders of various thermal capacities and radii. Recently, Rani [7] investigated the unsteady natural convection flow over a vertical cylinder with variable heat and mass transfer using the finite difference method.

All the above studies are confined to a fluid with constant physical properties, but when the free convective flows occur at high temperatures the viscosity effects on the flow cannot be neglected (Schlichting [8], Kakac et al. [9], Cengel [10]). Many processes in engineering occur at very high temperatures and, hence, the knowledge of viscosity effects on the convective heat transfer becomes very important for the design of the pertinent equipment. For instance, the viscosity of water increases by about 240% when the temperature decreases from 50 °C (μ=0.000548 kgm^{-1}s^{-1}) to 10 °C (μ=0.00131 kgm^{-1}s^{-1}) (Molla et al. [11]). To predict accurately the flow behavior, it is necessary to take into account this variation of viscosity. Also, the viscosity of a fluid is a measure of its resistance to the flow. After reasonable simplification, many researches studied the effect of viscosity on convective flows. Kafoussius and Rees [12] have investigated the effect of temperature-dependent viscosity on the mixed convection flow over a vertical flat plate. Gray et al. [13], Pop et al. [14], Kafoussias and Williams [15] and Elbashbeshy and Bazid [16] have shown that when the viscosity effect is included, the flow characteristics may be substantially changed compared to the constant viscosity case. Abo-Eldahab and El Gendy [17] studied variable viscosity effect on convective heat transfer in an electrically conducting fluid at a stretching surface. Hossain et al. [18] investigated the natural convection flow over a vertical wavy cone with variable viscosity, which depends linearly on the temperature. The above investigations found that the variation of viscosity with temperature is an interesting macroscopic physical phenomenon in fluid mechanics.

As generally less attention has been paid to the unsteady natural convection flow of a viscous incompressible fluid with variable viscosity over a heated vertical cylinder, the aim of the present work is to investigate the viscosity effects on the free convective flow of the air along a semi-infinite vertical cylinder. An empirical formula for the viscosity versus temperature presented in Cengel [10] and Touloukian et al. [19] is employed in the present study. The governing equations are solved numerically by the finite difference method to obtain the transient velocity, temperature, coefficient of skin-friction and heat transfer rate for different values of the viscosity parameter.

Section 2 begins with a detailed description about the formulation

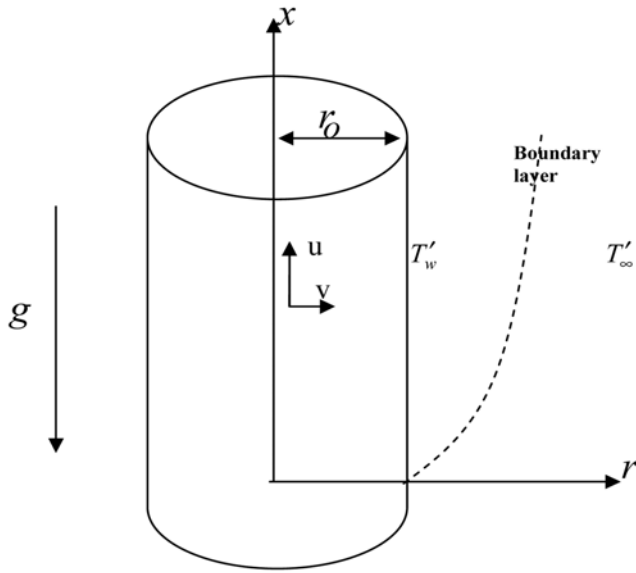†To whom correspondence should be addressed.
E-mail: cnkim@khu.ac.kr

Fig. 1. Schematic of the investigated problem.

of the problem. The conservation laws for mass, momentum and energy equations of the incompressible fluid flow past a semi-infinite vertical cylinder are discussed. In section 3 the details about the grid generation and numerical methods for solving the Navier-Stokes and energy equations are given. In section 4 the two-dimensional transient velocity and temperature profiles are analyzed for various values of viscosity-variation parameters. The average skin-friction and heat transfer rate are also elucidated. Finally, the concluding remarks are made.

FORMULATION OF THE PROBLEM

An unsteady two-dimensional laminar natural convection boundary layer flow of a viscous incompressible fluid past an isothermal semi-infinite vertical cylinder of radius r_0 is considered as shown in Fig. 1. The x-axis is measured vertically upward along the axis of the cylinder. The origin of x is taken to be at the leading edge of the cylinder, where the boundary layer thickness is zero. The radial coordinate r is measured perpendicular to the axis of the cylinder. The surrounding stationary fluid temperature is assumed to be of the ambient temperature (T'_∞). Initially, at time $t'=0$, it is assumed that the cylinder and the fluid are of the same temperature T'_∞. When $t'>0$, the temperature of the cylinder is maintained to be $T'_w (>T'_\infty)$, which gives rise to a buoyancy force. It is assumed that the effect of viscous dissipation is negligible in the energy equation.

With the above assumptions, the boundary layer equations governing the free convection flow over a vertical cylinder with Boussinesq's approximation can be expressed in the following form.

$$\frac{\partial(ru)}{\partial x} + \frac{\partial(rv)}{\partial r} = 0 \tag{1}$$

$$\frac{\partial u}{\partial t'} + u\frac{\partial u}{\partial x} + v\frac{\partial u}{\partial r} = g\beta(T'-T'_\infty) + \frac{1}{\rho r}\frac{\partial}{\partial r}\left(\mu r\frac{\partial u}{\partial r}\right) \tag{2}$$

$$\frac{\partial T'}{\partial t'} + u\frac{\partial T'}{\partial x} + v\frac{\partial T'}{\partial r} = \frac{\alpha}{r}\frac{\partial}{\partial r}\left(r\frac{\partial T'}{\partial r}\right) \tag{3}$$

where u and v are the velocity components parallel to x and r coordinates, respectively, g is the acceleration due to the gravity, β is the volumetric coefficient of thermal expansion, ρ is the density, α is the thermal diffusivity and $\mu\,(=\mu(T'))$ is the viscosity of the fluid depending on the temperature T' of the fluid.

The initial and boundary conditions are given by

$$\begin{aligned}
&t'\leq0:\ u=0,\ v=0,\ T'=T'_\infty\ \text{for all x and r}\\
&t'>0:\ u=0,\ v=0,\ T'=T'_w\ \text{at}\ r=r_0\\
&\qquad u=0,\ v=0,\ T'=T'_\infty\ \text{at}\ x=0\\
&\qquad u\rightarrow0,\ v\rightarrow0,\ T'\rightarrow T'_\infty,\ \text{as}\ r\rightarrow\infty
\end{aligned} \tag{4}$$

Now, the following non-dimensional quantities are introduced:

$$X=Gr^{-1}\frac{x}{r_0},\ R=\frac{r}{r_0},\ U=Gr^{-1}\frac{ur_0}{\upsilon},\ V=\frac{vr_0}{\upsilon},\ t=\frac{\upsilon t'}{r_0^2},\ T=\frac{T'-T'_\infty}{T'_w-T'_\infty},$$

$$Gr=\frac{g\beta r_0^3(T'_w-T'_\infty)}{\upsilon^2},\ Pr=\frac{\upsilon}{\alpha} \tag{5}$$

where $\upsilon(=\mu_\infty/\rho)$ is the reference kinematic viscosity, Gr and Pr denote the Grashof number and the Prandtl number, respectively.

Out of the many forms of viscosity variation available in the literature we have considered the following form presented in Cengel [10] and Touloukian et al. [19] for the air.

$$\mu(T')=a\frac{T'^{1/2}}{1+b/T'} \tag{6}$$

where a=1.458×10⁻⁶ kg/(m·s·K⁻¹ᐟ²), b=110.4 K. Eq. (6) is valid only for the pressure values between 0 and 10⁵ Pa.

$$\text{Let}\ \mu_\infty=a\frac{T'^{1/2}_\infty}{1+b/T'_\infty} \tag{7}$$

We can rewrite Eq. (6), as follows, by employing the Taylor series expansion and using Eq. (7).

$$\begin{aligned}
\mu(T')&=\mu(T'_\infty)+\frac{d\mu}{dT'}(T'-T'_\infty)+\frac{1}{2!}\frac{d^2\mu}{dT'^2}(T'-T'_\infty)^2+\cdots\\
&=a\frac{T'^{1/2}_\infty}{1+b/T'_\infty}\left[1+\left(\frac{1}{2T'_\infty}+\frac{bT'^{-2}_\infty}{(1+b/T'_\infty)}\right)(T'-T'_\infty)+O\{(T'-T'_\infty)^2\}\right]\\
&\cong\mu_\infty(1+\lambda(T'-T'_\infty))
\end{aligned}$$

where $\lambda=\frac{1}{2T'_\infty}+\frac{bT'^{-2}_\infty}{(1+b/T'_\infty)}$.

Let γ denote the non-dimensional viscosity parameter and be given by $\gamma=\lambda(T'_w-T'_\infty)$. Then the fluid viscosity in non-dimensional temperature is written as $\mu(T)=\mu_\infty(1+\gamma T)$.

By introducing the above non-dimensional quantities into the Eqs. (1)-(3), they are reduced to the following form.

$$\frac{\partial U}{\partial X}+\frac{\partial V}{\partial R}+\frac{V}{R}=0 \tag{8}$$

$$\frac{\partial U}{\partial t}+U\frac{\partial U}{\partial X}+V\frac{\partial U}{\partial R}=T+(1+\gamma T)\left(\frac{\partial^2 U}{\partial R^2}+\frac{1}{R}\frac{\partial U}{\partial R}\right)+\gamma\frac{\partial T}{\partial R}\frac{\partial U}{\partial R} \tag{9}$$

$$\frac{\partial T}{\partial t}+U\frac{\partial T}{\partial X}+V\frac{\partial T}{\partial R}=\frac{1}{Pr}\left(\frac{\partial^2 T}{\partial R^2}+\frac{1}{R}\frac{\partial T}{\partial R}\right) \tag{10}$$

The corresponding initial and boundary conditions in non-dimen-

sional quantities are given by

$$t\leq 0: U=0, V=0, T=0 \text{ for all } X \text{ and } R$$
$$t>0: U=0, V=0, T=1 \text{ at } R=1 \qquad (11)$$
$$\qquad U=0, V=0, T=0 \text{ at } X=0$$
$$\qquad U\rightarrow 0, V\rightarrow 0, T\rightarrow 0 \text{ as } R\rightarrow\infty$$

NUMERICAL SOLUTION OF THE PROBLEM

To solve the unsteady coupled non-linear governing Eqs. (8)-(10) an implicit finite difference scheme of Crank-Nicolson type has been employed. The finite difference equations corresponding to Eqs. (8)-(10) are as follows:

$$\frac{U_{i,j}^{k+1}-U_{i-1,j}^{k+1}+U_{i,j}^{k}-U_{i-1,j}^{k}}{2\Delta X}+\frac{V_{i,j}^{k+1}-V_{i,j-1}^{k+1}+V_{i,j}^{k}-V_{i,j-1}^{k}}{2\Delta R}$$
$$+\frac{V_{i,j}^{k+1}+V_{i,j}^{k}}{2[1+(j-1)\Delta R]}=0 \qquad (12)$$

$$\frac{U_{i,j}^{k+1}-U_{i,j}^{k}}{\Delta t}+\frac{U_{i,j}^{k}}{2\Delta X}(U_{i,j}^{k+1}-U_{i-1,j}^{k+1}+U_{i,j}^{k}-U_{i-1,j}^{k})$$
$$+\frac{V_{i,j}^{k}}{4\Delta R}(U_{i,j+1}^{k+1}-U_{i,j-1}^{k+1}+U_{i,j+1}^{k}-U_{i,j-1}^{k})=\frac{T_{i,j}^{k+1}+T_{i,j}^{k}}{2}$$
$$+\left(1+\gamma\frac{T_{i,j}^{k+1}+T_{i,j}^{k}}{2}\right)\left(\frac{U_{i,j-1}^{k+1}-2U_{i,j}^{k+1}+U_{i,j+1}^{k+1}+U_{i,j-1}^{k}-2U_{i,j}^{k}+U_{i,j+1}^{k}}{2(\Delta R)^2}\right.$$
$$+\left.\frac{U_{i,j+1}^{k+1}-U_{i,j-1}^{k+1}+U_{i,j+1}^{k}-U_{i,j-1}^{k}}{4[1+(j-1)\Delta R]\Delta R}\right)$$
$$+\gamma\frac{U_{i,j+1}^{k+1}-U_{i,j-1}^{k+1}+U_{i,j+1}^{k}-U_{i,j-1}^{k}}{4\Delta R}\frac{T_{i,j+1}^{k+1}-T_{i,j-1}^{k+1}+T_{i,j+1}^{k}-T_{i,j-1}^{k}}{4\Delta R} \qquad (13)$$

$$\frac{T_{i,j}^{k+1}-T_{i,j}^{k}}{\Delta t}+\frac{U_{i,j}^{k}}{2\Delta X}(T_{i,j}^{k+1}-T_{i-1,j}^{k+1}+T_{i,j}^{k}-T_{i-1,j}^{k})$$
$$+\frac{V_{i,j}^{k}}{4\Delta R}(T_{i,j+1}^{k+1}-T_{i,j-1}^{k+1}+T_{i,j+1}^{k}-T_{i,j-1}^{k})$$
$$=\frac{T_{i,j-1}^{k+1}-2T_{i,j}^{k+1}+T_{i,j+1}^{k+1}+T_{i,j-1}^{k}-2T_{i,j}^{k}+T_{i,j+1}^{k}}{2Pr(\Delta R)^2}$$
$$+\frac{T_{i,j+1}^{k+1}-T_{i,j-1}^{k+1}+T_{i,j+1}^{k}-T_{i,j-1}^{k}}{4Pr[1+(j-1)\Delta R]\Delta R} \qquad (14)$$

The region of integration is considered as a rectangle composed of the lines indicating $X_{min}=0$, $X_{max}=1$, $R_{min}=1$ and $R_{max}=16$ where R_{max} practically corresponds to $R=\infty$ which lies very far from the momentum and energy boundary layers. In the above Eqs. (12)-(14) the subscripts i and j designate the grid points along the X and R coordinates, respectively, where $X=i\Delta X$ and $R=1+(j-1)\Delta R$ and the superscript k designates a value of the time t ($=k\Delta t$), with ΔX, ΔR and Δt the mesh size in the X, R and t axes, respectively. To obtain an economical and reliable grid system for the computations, a grid independence test has been performed. The steady-state velocity and temperature values obtained with the grid system of 100× 500 differ in the second decimal place from those with the grid system of 50×250, and differ in the fifth decimal place from those with the grid system of 200×1,000. Hence the grid system of 100× 500 has been selected for all subsequent analyses, with $\Delta X=0.01$, $\Delta R=0.03$. Also, the time step size dependency has been carried out, which yields $\Delta t=0.005$ for reliable result.

From the initial conditions given in Eq. (11), the values of velocity U, V and temperature T are known at time t=0; then the values of T, U and V at the next time step can be calculated. Generally, when the above variables are known at $t=k\Delta t$, the value of the variables at $t=(k+1)\Delta t$ are calculated as follows. The finite difference Eqs. (13) and (14) at every internal nodal point on a particular i-level constitute a tri-diagonal system of equations. Such a system of equations is solved by Thomas algorithm (Carnahan et al. [20]). At first, the temperature T is calculated from Eq. (14) at every j nodal point on a particular i-level at the (k+1)th time step. By making use of these known values of T, the velocity U at the (k+1)th time step is calculated from Eq. (13) in a similar manner. Thus the values of T and U are known at a particular i-level. Then the velocity V is calculated from Eq. (12) explicitly. This process is repeated for the consecutive i-levels. Thus the values of T, U and V are known at all grid points in the rectangular region at the (k+1)th time step. This iterative procedure is repeated for many time steps until the steady-state solution is reached. The steady-state solution is assumed to have been reached when the absolute difference between the values of velocity as well as temperature at two consecutive time steps is less than 10^{-5} at all grid points.

The truncation error in the employed finite-difference approximation is $O(\Delta t^2+\Delta R^2+\Delta X)$ and tends to zero as ΔX, ΔR and $\Delta t\rightarrow 0$. Hence, the system is compatible. Also, as explained by Ganesan and Rani [21], unconditionally stable is the finite difference scheme on this type of problems where the velocity U is non-negative and the velocity V is non-positive. Stability and compatibility ensures convergence. The computations for the current problem have been carried out on an Intel Pentium 4 CPU 3.20 GHz computer system for different values of γ.

RESULTS AND DISCUSSION

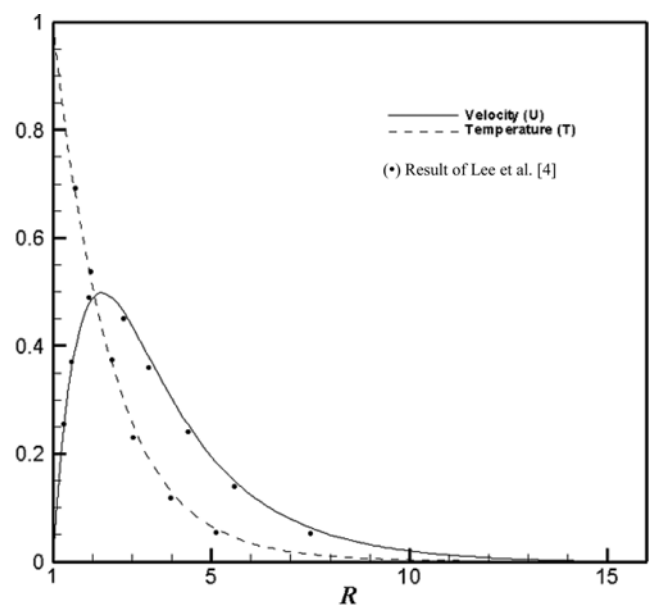To validate the current numerical procedure, the present simu-

Fig. 2. Comparison of the velocity and temperature profiles for Pr=0.7 and γ=0.0.

Table 1. The values of viscosity-variation parameter γ and the Prandtl number based on assumed temperatures at the wall and the surrounding fluid [22]

T'_∞ (K)	λ (K^{-1})	T'_w (K)	$\gamma=1$ $(T'_w-T'_\infty)$	Pr at T'_∞ (K)	Pr at T'_w (K)	$Pr(T'_w)/$ $Pr(T'_\infty)$
240	$\approx 3.34\times10^{-3}$	390	≈ 0.5	0.723	0.692	0.957
		340	≈ 0.3		0.701	0.970
273	$\approx 2.87\times10^{-3}$	418	≈ 0.4	0.714	0.689	0.965
		373	≈ 0.3		0.695	0.973
373	$\approx 1.95\times10^{-3}$	523	≈ 0.25	0.695	0.684	0.984
		473	≈ 0.2		0.685	0.986
473	$\approx 1.46\times10^{-3}$	573	≈ 0.1	0.685	0.684	0.999

lated velocity and temperature profiles are compared with the results of Lee et al. [4] for the steady-state, isothermal and constant viscosity with Pr=0.7. The comparison results, which are shown in Fig. 2, are found to be in good agreement.

The normalized viscosity can be written as

$$\mu(T)/\mu_\infty = 1+\gamma T \qquad (15)$$

From the above Eq. (15) it can be noted that when $\gamma>0$ the viscosity of the fluid increases with the increase in the temperature and it is factual for gases.

In Table 1, the calculated values of γ and the Prandtl numbers from the physically feasible wall and ambient temperatures are tabulated. It can be observed from Table 1 that the value of γ can be as large as 0.5, which means that the value of $(1+\gamma T)$ can vary from 1.0 to 1.5 in the flow field. In the present numerical simulations three values of γ are chosen: 0.0, 0.25 and 0.5. Also, for each feasible difference of the wall and ambient temperatures it can be said that the variation of the Prandtl number with temperature is not noticeable within 5% of the value of the reference Prandtl number. Therefore, the nondimensionalized system of the Eqs. (8)-(10) with the nondimensional conditions given by Eq. (11) can be solved with a

fixed value of the Prandtl number. In the succeeding subsections the simulated transient behavior of the dimensionless velocity, temperature, average skin-friction coefficient and heat transfer rate for varying γ are discussed in detail with Pr=0.7 (air).

1. Velocity

Fig. 3 depicts the variations of simulated transient dimensionless velocity (U) at different locations for different γ against the time (t). It is observed that at all locations the velocity increases with time, reaches the temporal maximum, then decreases and at last reaches the asymptotic steady-state. For example, when γ=0.25 and (X, R)=(1.0, 2.20), the velocity increases with time monotonically from zero and reaches the temporal maximum (U=0.495) at t=4.89, then slightly decreases with time and becomes asymptotically steady (U= 0.485). The nonlinear feature of the unsteady momentum equation together with the finite values of nondimensional viscosity (1+γT) and nondimensional thermal diffusivity 1/Pr is believed to cause the overshoot in the figure. It is also observed that transient velocity decreases with the increasing viscosity-variation parameter.

Fig. 4 shows the graphical representation of the simulated transient velocity profiles at the temporal maximum and steady-state against the radial coordinate R at X=1.0 for different γ. It is observed that the velocity profiles start with the value zero at the wall, reach their maximum close to the hot wall and then monotonically decrease to zero. Clearly, the time to reach the temporal maximum of velocity increases with the increasing viscosity-variation parameter γ, while the times to reach the steady-state are almost the same for different γ. Here, it is observed that the magnitude of the peak velocity gets smaller as the viscosity-variation parameter becomes larger. The increasing values of the viscosity-variation parameter increase the velocity of the flow away from the wall, because the viscosity is increasing with the increase of the viscosity-variation parameter. The position of the maximum velocity gets farther from the cylinder wall for higher values of γ. This qualitative effect arises because, for the case of fluid with larger viscosity (say, γ=0.5), the fluid is not able to move easily in a region very near the heated surface,
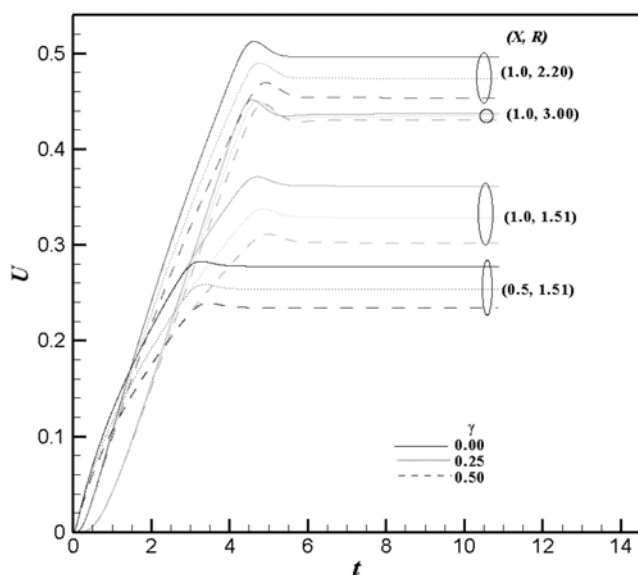

Fig. 3. Variation of the transient velocity for different values of γ with time.
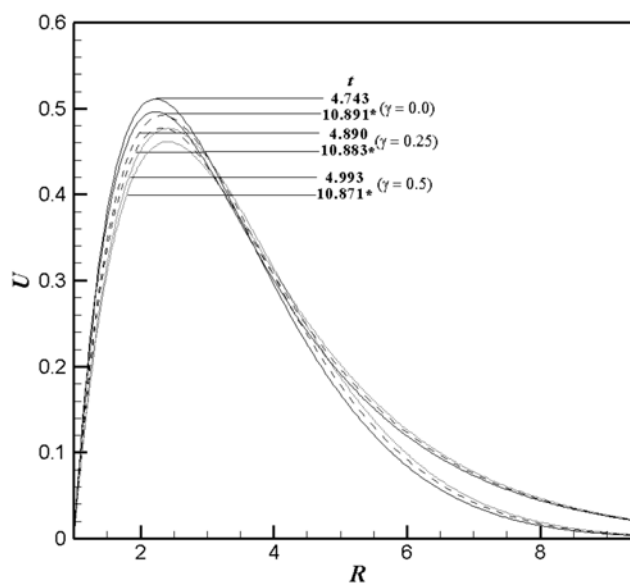

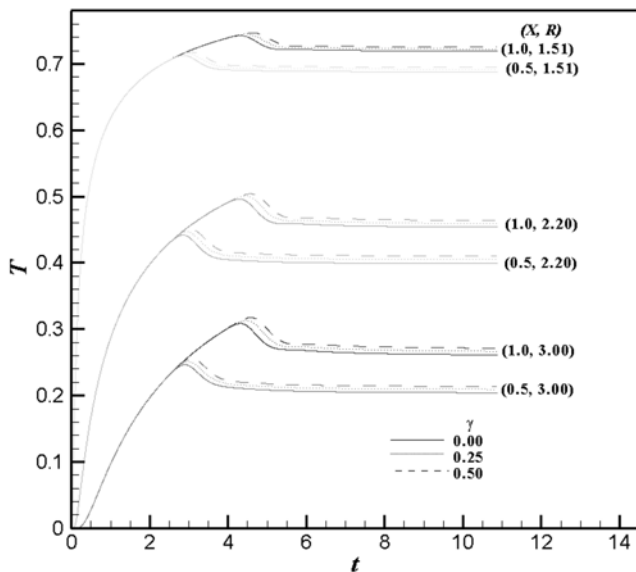**Fig. 4. Variation of the velocity profiles with respect to γ at X=1.0 (*-- Steady-state).**

Fig. 5. **Variation of the transient temperatures for different values of γ with time.**

Fig. 6. **Variation of the steady-state temperature profiles with respect to γ at X=1.0.**

while the fluid with smaller viscosity (say, γ=0.5) can move more freely near the wall. From the above results, it is obvious that neglecting the variation of fluid viscosity, which depends on the temperature, introduces a substantial error.

2. Temperature

The simulated transient temperature with respect to γ at different locations is plotted against the time in Fig. 5. At all the locations the transient temperature profiles increase with time, reach the temporal maximum, decrease and attain the steady-state asymptotically. At the beginning, the temperature profiles at different axial locations along the axial coordinate coincide with each other and then bifurcate with small temperature difference caused by different values of γ. The temporal overshoot of the temperature is more noticeable at higher values of the axial position.

In the transient period, the nature of transient temperature profiles with respect to γ is particularly noticeable. The transient temperature profiles of fluids with variable viscosity (i.e., γ>0), initially coincide with and then deviate from the temperature profiles of fluids with constant viscosity (i.e., γ=0). For example, the temperature profiles of γ=0.5 and 0.25 at the location (X, R)=(1.0, 2.20) deviate from the temperature profile of the fluid with constant properties (i.e., γ=0), say, for t≥4.0. Hence, it can be noticed that, in the beginning of the transient period, the fluid with variable viscosity (γ> 0) follows the characteristics of fluid with constant viscosity (γ=0). Also, the maximum temperature value increases with the increasing γ.

The simulated steady-state temperature profiles for different γ at X=1.0 against the radial coordinate are shown in Fig. 6. The temperature profiles start with the hot wall temperature (T=1) and then monotonically decrease to zero as the radial coordinate increases. The temperature profiles are observed to be increasing with the increase of the viscosity-variation parameter. It is related to the fact that with the increase in the viscosity-variation parameter the viscosity of the fluid is increasing, which allows higher velocity away from the hot wall.
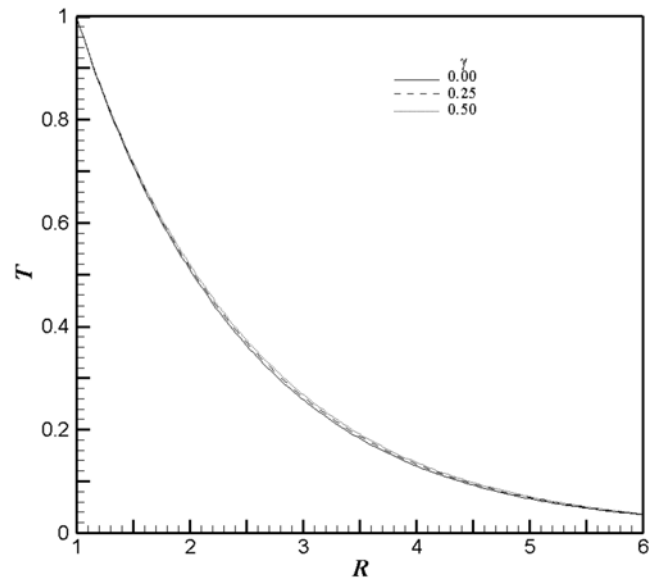
The temperature profiles increase with increasing γ, which is associated with the fact that the increase in γ yields the decrease in the peak velocity as shown in Fig. 4. However, two opposing effects of the increase in γ on the fluid particle can be considered. The first effect decreases the velocity of the fluid particle due to the increase in the viscosity and the second effect increases the velocity of the fluid particle due to the increase in the temperature as shown in Fig. 6. Near the cylinder wall (say, 1≤R≤4) the temperature is relatively high; consequently, the first effect will be dominant and the velocity decreases as γ increases (Fig. 4). On the other hand, far from the cylinder wall (say, R≥4), where the temperature T is relatively low, the second effect will be dominant and the velocity increases as γ increases (Fig. 4).

3. Average Skin-friction Coefficient and Heat Transfer Rate

Knowing the unsteady behavior of velocity and temperature profiles, it is worth to study the average skin-friction coefficient and the average heat transfer rate (Nusselt number). The friction coefficient is an important parameter in the heat transfer studies since it is directly related to the heat transfer coefficient. The increased skin friction is generally a disadvantage in technical applications, while the increased heat transfer can be exploited in some applications such as heat exchangers, but should be avoided in others such as gas turbine applications, for instance.

The shear stress at the wall can be expressed as

$$\tau_w = \left(\mu \frac{\partial u}{\partial r} \right)_{r=r_0} \tag{16}$$

By introducing the non-dimensional quantities given in Eqs. (7) and (15) in the above Eq. (16), we get

$$\tau_w = \frac{\mu_\infty^2 \mathrm{Gr}}{\rho r_0^2} \left((1+\gamma T) \frac{\partial U}{\partial R} \right)_{R=1} \tag{17}$$

Considering $(\mu_\infty^2 \mathrm{Gr})/(\rho r_0^2)$ to be the characteristic shear stress, then the skin-friction coefficient can be written as

$$C_f = \left((1+\gamma T)\frac{\partial U}{\partial R} \right)_{R=1} \tag{18}$$

The integration of the Eq. (18) from X=0 to X=1 gives the following average skin-friction coefficient.

$$\overline{C}_f = (1+\gamma)\int_0^1 \left(\frac{\partial U}{\partial R}\right)_{R=1} dX \tag{19}$$

The Nusselt number can be written as follows:

$$Nu_x = \frac{\dot{q}_w}{k_\infty(T'_w - T'_\infty)/r_0} \tag{20}$$

where the heat transfer $\dot{q}_w = -k\left(\dfrac{\partial T'}{\partial r}\right)_{r=r_0} = -k_\infty\dfrac{T'_w - T'_\infty}{r_0}\left(\dfrac{\partial T}{\partial R}\right)_{R=1}$.

Thus, Eq. (20) can be written as

$$Nu_X = -\left(\frac{\partial T}{\partial R}\right)_{R=1} \tag{21}$$

The integration of the above Eq. (21) with respect to X yields the following average Nusselt number:

$$\overline{Nu} = -\int_0^1 \left(\frac{\partial T}{\partial R}\right)_{R=1} dX \tag{22}$$

The derivatives involved in the Eqs. (19) and (22) are evaluated using a five-point approximation formula and then the integrals are evaluated using Newton-Cotes closed integration formula. The simulated average non-dimensional skin friction coefficient and heat transfer rate for different γ have been plotted against the time in Fig. 7. From the figure it is observed that for all values of γ the average skin friction coefficient increases with time, attains the temporal maximum value, and after slight decreasing, becomes asymptotically steady. For increasing values of γ the average skin-friction increases in association with the fact that the increase in the value of γ yields

Fig. 7. Variation of the average skin friction and Nusselt number with respect to γ.

the increase in the viscosity near the wall.

From Fig. 7 with the increase of the viscosity-variation parameter γ the average heat transfer rate decreases monotonically, which is in line with the fact that the increase in the viscosity-variation parameter leads to the decrease in the velocity near the wall (shown in Fig. 4) and the increase in the temperature (shown in Fig. 6). Also, the Nusselt numbers for different values of γ decrease with time at the beginning, reach the temporal minimum, and then after slight increasing, reach the steady-state. For different values of γ there is little difference in the average Nusselt number in the very early part of the transient period. This fact reveals that initially the heat transfer is performed mostly by the conduction with large temperature difference between the wall and the fluid. As time increases, the free convection effect becomes more pronounced and, therefore, the local Nusselt number generally decreases, reducing the heat transfer rates.

CONCLUSIONS

A numerical study has been performed for the unsteady natural convection along a semi-infinite vertical cylinder. The viscosity of the fluid is assumed to be temperature dependent, while the Prandtl number is kept constant. An empirical formula for temperature-dependent viscosity of the air proposed in the existing literature is employed in the present study. A Crank-Nicolson type of implicit method is used to solve the dimensionless governing equations in a meridian plane. The computations are carried out to study the influence of the viscosity-variation parameter, γ on the transient dimensionless velocity, temperature, skin friction coefficient and heat transfer rate. From the present numerical analysis the following observations are noted.

Velocity profiles near the wall decrease with the increasing γ, while temperature profiles increase. The time elapsed to reach the temporal maximum of the velocity increases with the increasing γ. Initially, the unsteady behavior of the temperature with variable viscosity ($\gamma>0$) coincides with that of the fluid with constant properties ($\gamma=0$). Then the temperature with variable viscosity ($\gamma>0$) deviates from that with constant properties ($\gamma=0$) and reaches the steady-state asymptotically. When the viscosity-variation parameter is larger, lower velocity near the isothermal cylinder wall and higher velocity in a region away from the wall are observed, which gives lower average Nusselt number. The increase in the viscosity-variation parameter leads to the decrease in the average heat transfer rate and to the increase in the average skin friction.

From the present study, it is observed that the results pertaining to the variable viscosity differ significantly from those of constant viscosity. The viscosity of a working fluid has turned out to be sensitive to the variation of temperature in a natural convection problem. Hence, the effect of variable viscosity has to be taken into consideration in order to predict the skin friction factor and heat transfer rate accurately.

REFERENCES

1. E. M. Sparrow and J. L. Gregg, *Trans. of ASME*, **78**, 1823 (1956).
2. W. J. Minkowycz and E. M. Sparrow, *J. Heat Trans*., **96**, 178 (1974).
3. T. Fujii and H. Uehera, *Int. J Heat Mass Trans*., **13**, 607 (1970).
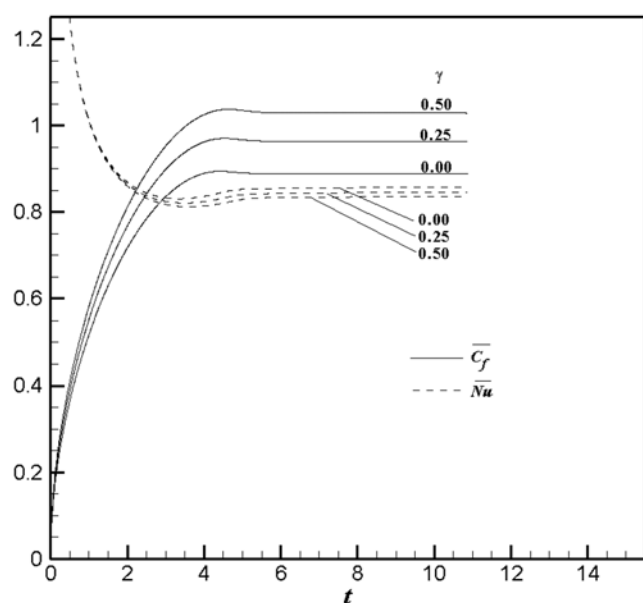4. H. R. Lee, T. S. Chen and B. F. Armaly, *J. Heat Trans*., **110**, 103

(1988).

5. R. P. Dring and B. Gebhart, *J. Heat Trans.*, **88**, 246 (1966).

6. K. Velusamy and V. K. Garg, *Int. J. Heat Mass Trans.*, **35**, 1293 (1992).

7. H. P. Rani, *Heat and Mass Trans.*, **40**, 67 (2003).

8. H. Schlichting, *Boundary layer theory*, McGraw-Hill, New York (1979).

9. S. Kakac, R. K. Shah and W. Aung, *Handbook of single-phase convective heat transfer*, John Wiley & Sons, New York (1987).

10. Y. Cengel, *Fluid Mechanics fundamentals & applications*, McGraw-Hill, New York (2006).

11. M. M Molla, M. A. Hossain and R. S. R. Gorla, *Heat Mass Trans.*, **41**, 594 (2005).

12. N. G Kafoussius and D. A. S. Rees, *Acta Mechanica.*, **127**, 39 (1998).

13. J. Gray, D. R. Kassory and H. Tadjeran, *J. Fluid Mech.*, **117**, 233 (1982).

14. I. Pop, R. S. R. Gorla and M. Rashidi, *Int. J. Eng. Sci.*, **30**, 1 (1992).

15. N. G. Kafoussias and E. W. Williams, *Int. J. Eng. Sci.*, **33**, 1369 (1995).

16. E. M. A. Elbashbeshy and M. A. A. Bazid, *J. Phys. D: Applied Physics*, **33**, 2716 (2000).

17. E. M. Abo-Eldahab and El. Gendy, *Phys. Scripta*, **62**, 321 (2000).

18. M. A. Hossain, M. S. Munir and I. Pop, *Int. J. Thermal Sci.*, **40**, 366 (2001).

19. Y. S. Touloukian S. C. Saxena and P. Hestermans, *Thermophysical properties of matter*, Viscosity, The TPRC Data Series, Plenum, New York (1975).

20. B. Carnahan, H. A. Luther and J. O. Wilkes, *Applied numerical methods*, John Wiley & Sons, New York (1969).

21. P. Ganesan and H. P. Rani, *Heat Mass Trans.*, **33**, 449 (1998).

22. F. P. Incropera and D. P. Dewitt, *Fundamentals of heat and mass transfer*, John Wiley & Sons, New York (2007).